Effect of chain length and topological constraints on segmental relaxation in cyclic PDMS

Journal:	*Macromolecules*
Manuscript ID	Draft
Manuscript Type:	Article
Date Submitted by the Author:	n/a
Complete List of Authors:	Arrighi, Valeria; Heriot-Watt University, Institute of Chemical Sciences Gagliardi, Simona; Heriot-Watt University, Institute of Chemical Sciences Ganazzoli, Fabio; Politecnico di Milano, Dip. Chimica, Materiali ed Ingegneria Chimica "G. Natta" Higgins, Julia; Imperial College, Chem Eng Raffaini, Giuseppina; Politecnico di Milano, Dept. Chimica Materiali ed Ing. Chimica "G. Natta" Tanchawanich, Jeerachada; Esso (Thailand) Taylor, Jenny; Heriot-Watt University, Institute of Chemical Sciences Telling, Mark; Rutherford Appleton Lab, ISIS

Effect of chain length and topological constraints on segmental relaxation in cyclic PDMS

Valeria Arrighi[a], *Simona Gagliardi*[a], *Fabio Ganazzoli*[b], *Julia S. Higgins*[c], *Giuseppina Raffaini,*[b]

Jeerachada Tanchawanich[a,d], *Jenny Taylor*[a], *Mark T.F. Telling*[e,f]

[a] Institute of Chemical Sciences, School of Engineering and Physical Science, Heriot- Watt University, Edinburgh, EH14 4AS, United Kingdom

[b] Dipartimento di Chimica, Materiali e Ingegneria. Chimica ''Giulio Natta'', Politecnico di Milano, via L. Mancinelli 7, 20131, Milano, Italy; E-mail: fabio.ganazzoli@polimi.it; Fax: +39-02-2399-3080; Tel: +39-02-2933-3024

[c] Chemical Engineering Department, Imperial College London, South Kensington Campus London SW7 2AZ, UK; E-mail: j.higgins@imperial.ac.uk

[d] Present Address: Esso (Thailand), Thoongsukla, Sriracha, Chonburi 20230 Thailand; *E-mail*: Jeerachada.tanchawanich@exxonmobil.com

[e] ISIS, Rutherford Appleton Laboratory, Chilton, Didcot, OX11 OQX, United Kingdom

[f] Department of Materials, University of Oxford, Parks Road, Oxford, OX1 3PH, United Kingdom

CORRESPONDING AUTHOR:

Valeria Arrighi, fax: +44 (0) 131 451 3180; phone: +44 (0) 131 451 3108, v.arrighi@hw.ac.uk

ABSTRACT.

We present a detailed investigation of local dynamics of linear and cyclic poly(dimethyl siloxane) (PDMS) covering a wide range of molar masses. To aid interpretation of the experimental data, QENS measurements in the time scale from 2 to 200 ps and at Q = 0.3 to 1.8 $Å^{-1}$ are complemented by theoretical calculations. These make use of a methodology developed by us elsewhere, applicable to both simple chain modes and real chains, and applied here, for the first time, to cyclic PDMS.

Analysis of the incoherent dynamic structure factor at $T < T_m$, shows that the rotational motion of the methyl groups is unaffected by polymer topology. At higher temperatures, the QENS data are described by a model that consists of two dynamic contributions: methyl group rotation and segmental motion, the latter described by a stretched exponential function.

Relaxation times of both linear and cyclic PDMS increase with increasing molar mass. Several features predicted by theory are also reproduced by the experimental data. We show, unambiguously, that rings have higher relaxation times for the segmental motion compared to linear chains of the same number of monomer units. Theoretical calculations support the idea that such slowing down of local dynamics is due to the topological constraint imposed by the ring closure, a constraint which becomes negligible for very large molar masses.

Our calculations suggest that, due to its albeit small conformational rigidity, PDMS undergoes an additional constraint which further increases the relaxation time, producing a shallow maximum for N ≈ 50 repeat units. A similar feature is also observed in the experimental QENS data.

Values of activation energy, E_a, are derived from analysis of the temperature dependence of the quasielastic broadening and are found to be in agreement with viscosity measurements reported in the literature. Although the pronounced molar mass dependence of E_a for linear PDMS is certainly linked to the presence of mobile chain ends, for the cyclic polymers the behavior appears to be more complex than anticipated.

KEYWORDS. poly(dimethyl siloxane), quasi-elastic neutron scattering, segmental motion, cyclic polymers, rheology.

1. INTRODUCTION

Cyclic polymers differ from linear chains by one single bond that links the chain ends. This apparently trivial topological constraint has a profound effect on many polymer properties[1]. For example, it has been shown to influence crystallisation[2-4], thermal properties such as heat capacity[5] and glass transition[4, 6-9], bulk viscosity[10-12] and diffusion coefficients[13-16].

Early theoretical studies focused on the effect of polymer topology on conformation and radii of gyration[17-20], glass transition and dynamics[21]. Extensive work has also been carried out using computer simulations[22-29]. Experiments on well characterized cyclic molecules have made it possible to confirm theoretical predictions of chain dimension in solution[17, 19, 30-35] and in bulk[36-39], leading to a good understanding of their structural properties. Recently, good agreement between theory and experiments was reported by us for cyclic poly(dimethyl siloxane)s (PDMS) in the undiluted state. Our results showed that highly flexible cyclic polymers in the melt adopt an even more compact conformation than that of unperturbed rings, leading to that $R_g \propto M_w^{0.4}$.[36, 37]

In this work we make a comparison between linear and cyclic PDMS dynamics. Although macroscopic properties such as bulk viscosity[10-12] and diffusion coefficients[13-16] have been well documented in the literature, fewer studies have addressed microscopic behaviour. Here, using quasi-elastic neutron scattering (QENS) we aim to provide a microscopic insight into the different dynamic behaviour of linear and cyclic molecules, within length scales that are sensitive to molecular structure.

Experimental and theoretical studies of melt dynamics have focused on the extent to which chain ends, or better absence of, affect the dynamic behavior of a polymer[21]. Chain motion in a dense solution or melt of entangled linear or branched chains is well understood in terms of the reptation model.[40-43] However, the concept of reptation is strictly correlated with the existence of chain ends and for this reason this type of motion should be strongly suppressed in non-linear polymers such as stars or closed ring molecules[21, 44].

Early viscoelastic measurements of cyclic polystyrene produced contradictory results, particularly with regard to the molecular weight dependence of the viscosity, and this has been largely attributed to contamination of linear chains and/or formation of knots.[32, 45, 46] More recently, Kapnistos et al.[47] reported that high purity cyclic polystyrenes (PS) with M_w above the

entanglement molecular weight for linear PS show no obvious rubbery plateau but a power-law stress relaxation.

Generally, theoretical predictions of significant differences between the melt dynamics of linear and cyclic polymers have not been fully supported by experiments. The zero-shear rate viscosities of cyclic polystyrenes in the molten state was found to be lower compared to values measured for linear chains, the maximum difference being approximately a factor of 2 at low molecular weight.[48] However, what was surprising is that the molecular weight dependence of cyclics showed the two-power law regimes observed for linear polymers due to a transition from unentagled to entangled behaviour. For both PS and PDMS[10-12], the crossover occurred at similar values of critical molecular weight M_c indicating qualitatively similar dynamic behaviour for rings and linear polymers.

On the basis of rheological data, diffusion should be faster for rings than their linear counterpart. This is in agreement with computer simulations which indicate that topological interactions greatly influence melt dynamics leading to faster diffusion for melts of rings and faster relaxation times compared to linear chains of equal mass[22-29]. Only limited experimental studies on the molecular motion of cyclic molecules have been reported. Among these, interdiffusion experiments of bilayers consisting of cyclic PS and deuterated cyclic PS have shown faster mutual diffusion compared to equivalent bilayers of linear chains[49]. Diffusion coefficients of cyclic PS were reported to be twice those of the corresponding linear molecules, at all temperatures and above the entanglement molecular weight. Similarly, the rheological measurements of Bras *et al.*[38] on linear and cyclic poly(ethylene oxide) (PEO) show that the viscosity of the ring melt is a factor of 2 lower compared to values for the linear chains, as expected given that this is equal to the ratio between their radii of gyration. However, linear and ring polymers are reported to have the same activation energies indicating that the temperature dependence of the segmental friction does not depend on polymer topology. These authors note that this result is consistent with an earlier observation of the same shift factors of entangled linear and ring polymers.[47]

When comparing viscosity, η, at the same distance from the glass transition temperature i.e. at iso-frictional conditions, values are usually found to be lower for rings than for the corresponding linear chains. This has been observed in a number of systems including

polystyrene[48], [33], polybutadiene[50] and poly(oxy ethylene)[51]. As discussed in a recent review[52], two regimes can be identified: (a) at low molecular weights, for unentangled chains, the ratio between the viscosity of linear chains and rings, η_l/η_r is constant and equal to 2 but (b) above the entanglement molecular weight it increases above this value depending on the number of entanglements.

As already mentioned, for the polymer investigated here, PDMS, bulk viscosity measurements identified a cross-over region[10-12] with η_r being higher than η_l at low molar mass but smaller at high molecular weight. This behaviour could not be simply attributed to chain end effects and was still evident even after scaling at constant segmental mobility. Semlyen et al. argued that configurational restrictions in the ring molecules would be responsible for a reduction in segmental mobility, resulting in higher viscosity[10-12].

Following previous studies, including our own work[53-56], here we present a systematic investigation of the influence of topology on local chain motion by comparing QENS data of linear and cyclic PDMS. The local dynamics of PDMS has been investigated extensively by neutron scattering[55-57] and other experimental techniques such as dielectric spectroscopy[58-61] as well as simulations[62]. Most of these studies have dealt with linear high molecular weight chains and there is little in the literature on the comparison between cyclic and linear PDMS dynamics, except for QENS measurements reported by Allen *et al*.[54, 63]**.** Although these were limited to linear and cyclic PDMS samples with degree of polymerisation less than 20 (equivalent to $M_n \leq$ 1500 g mol^{-1}), the diffusion coefficients extracted from the quasi-elastic broadening showed that linear chains are faster than the small rings, the difference becoming more pronounced with decreasing molecular weight.

The results presented in the following sections cover a much wider range of molar mass and we present a detailed analysis of the incoherent dynamic structure factor, including temperature and Q dependence. The experimental data are supplemented by theoretical calculations using a methodology developed by us elsewhere applicable to both simple chain modes and real chains.[53] The same methodology is extended here, for the first time, to cyclic PDMS.

2. EXPERIMENTAL METHODS AND THEORETICAL APPROACH

2.1 Materials

Table 1 gives a list of samples used for the neutron scattering measurements. The linear PDMS samples, with trimethylsiloxy terminal groups, are commercial materials from Dow Corning Ltd. The molecular weights of these linear samples, except for L162 and L237, were obtained from the manufacturer and are consistent with values reported by Cowie et al. for silicone fluids of comparable viscosity[64]. Cyclic PDMS samples were provided by Dr. J. A. Semlyen and Prof. P. Griffiths except for C370 and C445 that were purchased from Sigma-Aldrich. L1460 was also kindly supplied and characterized by Dr. J. A. Semlyen and coworkers. Number-average molar masses, M_n, and polydispersities (M_w/M_n) of the cyclic siloxanes as well as values for L1400 were obtained by Semlyen and coworkers using gel permeation chromatography calibrated using standard siloxane samples.

2.2 Thermal Properties: T_g and Crystallisation

The molecular weight dependence of the glass transition temperature, T_g, of both linear and cyclic PDMS has been reported in the literature[4, 64]. A linear relationship between T_g and M_n^{-1} was observed for both linear and cyclic PDMS but whilst the former has a negative slope (-6.5×10^3 K g mol^{-1}) the latter displays a positive slope (3.6×10^3 K g mol^{-1})[4]. Glass transitions listed in Table 1 have been derived from the known molar mass dependence reported in the literature[4, 64]. In agreement with experiments[4, 64] as well as theoretical predictions[6], for chains of similar length, the T_g of the rings is always at higher temperature compared to that of linear chains.

To determine the lower temperature at which QENS experiments can be performed, the melting temperature, T_m, of the linear and cyclic samples were measured using a TA Instruments differential scanning calorimeter (DSC 2010) with both heat flow and temperature scales calibrated against indium metal. DSC measurements were carried out under a nitrogen flow at a heating rate of 10^{o}C min^{-1}. T_m values for semi-crystalline samples are reported in Table 1. Our results are in good agreement with the work of Clarson et al.[4] who demonstrated that cyclic

siloxanes with number-average repeat units, N_n, in the range $12 \leq N_n \leq 40$ ($890 \leq M_n \leq 2930$) as well as linear chains with $6 \leq N_n < 21$ ($530 \leq M_n \leq 1645$) do not crystallize.

Table 1 – Molar mass and thermal transitions of linear (L) and cyclic (C) PDMS.

Code	η_k[(1)] / cSt	M_n /g mol^{-1}	M_w/M_n	T_g /K	T_m /K
L162	0.65	162	-	110	210
L237	1	237	-	125	190
L550	3.0	550	-	136	-
L1400	----	1430[(2)]	1.02	145	-
L2000	20	2,000		148	-
L3780	50	3,780		149	220,235
L9430	200	9,430		149	220,235
C370	----	370	-	165	227
C445	----	445	-	157	270
C1200		1,218[(2)]	1.08	152	-
C2700		2,675[(2)]	1.03	151	-
C19000		19,000[(3)]	-	150	229,239

[(1)]: kinematic viscosity in cSt, as reported by manufacturer at 25^{o}C.

[(2)]: supplied and characterized by Dr. J. A. Semlyen and Prof. P. Griffiths.

[(3)]: average number of repeat units, $N_n = 257$

2.3 Neutron Scattering Measurements

Quasielastic neutron scattering experiments were carried out on the high energy resolution back scattering spectrometers IRIS and OSIRIS (ISIS, Rutherford Appleton Laboratory, UK) using the PG002 (offset) analyser configuration, which gives energy resolutions (measured as FWHH)

of 17.5, and 24.5 μeV for IRIS and OSIRIS, respectively. This energy resolution affords access to a temporal range spanning ca. 2 – 200 ps. The energy range covered in all experiments was –0.2 to 1.0 meV and the Q range varied from 0.5 to 1.8 $Å^{-1}$. Hollow cylinders were used to contain the liquid samples during the IRIS and OSIRIS measurements. Sample's thickness was less than 0.25 mm, corresponding to a transmission of more than 90% of the incident neutron beam. At this level multiple neutron scattering effects were deemed negligible

For each sample, at least one set of QENS data were collected at 110 degrees above the respective T_g. To explore the temperature dependence of the dynamics, one of the linear siloxanes (L550) and all of the cyclic samples were measured at selected temperatures above their T_g. In addition to this, for a few cyclics, QENS spectra were recorded below the polymer T_g.

In a QENS experiments, the scattered intensity is measured as a function of both energy and momentum transfer, Q (= $(4\pi/\lambda)\sin(\theta/2)$, where λ is the neutron wavelength and θ is the scattering angle). The dynamic incoherent structure factor, $S(Q,\omega)$, is determined from time-of-flight data, after removing empty cell contributions and correcting for absorption, using standard software available at ISIS.

$S(Q,\omega)$ is related to the double differential scattering cross section, $\partial^2\sigma/(\partial E\, \partial\Omega)$ which represents the probability that a neutron is scattered with energy change ΔE into the solid angle $\Delta\Omega$. For neutrons scattered incoherently,

$$\left(\frac{\partial^2\sigma}{\partial\Omega\,\partial E}\right)_{inc} = \frac{Nk}{k_o}\Delta b^2\, S_{inc}(Q,\omega) \qquad (1)$$

where N is the number of atoms, and k, k_o represent the magnitude of the scattered and incident wave vectors (k= $2\pi/\lambda$), respectively. The term Δb^2 depends on fluctuations of the scattering length b due to the presence of different isotopes and it is related to the incoherent cross section (σ_{inc}= $4\pi\ \Delta b^2$).

For PDMS, σ_{inc} = 481.6 barns which is much larger than the coherent cross section of the repeat unit, σ_{coh}(H)= 28.4 barn. As a result, coherent scattering is negligible and, as stated by (1), the total scattering cross section is approximated to the incoherent scattering cross section; hence the subscript "inc".

The incoherent scattering law, $S_{inc}(Q,\omega)$, is defined as the time- Fourier transform of the intermediate scattering function $I_{inc}(Q,t)$:

$$S_{inc}(Q,\omega) = \frac{1}{2\pi}\int I_{inc}(Q,t)\exp(-i\omega t)\,dt \qquad (2)$$

which describes correlations between the positions of the same scattering nuclei at time zero and t: $I_{inc}(Q,t) = \frac{1}{N}\sum < \exp(iQ\cdot R_i(t))\exp(-iQ\cdot R_i(0))>$

(3)

where the brackets indicate a thermal average and $R_i(t)$ and $R_i(0)$ represent the position of the i-th nucleus (i=1, 2, …, N) at time t and t=0, respectively. Thus, $S_{inc}(Q,\omega)$ gives dynamic information on self, rather than collective, correlations in the system under study.

Generally, the measured dynamic incoherent structure factor is a convolution of different processes $S_{inc}(Q,\omega) = S_{inc}^{trans}(Q,\omega)\otimes S_{inc}^{rot}(Q,\omega)\otimes S_{inc}^{vib}(Q,\omega)$

(4)

i.e. vibrations (vib), rotations (rot) and translations (trans) of the scattering centers. Similarly, the intermediate scattering function can be written as the product of the different dynamic contributions:

$$I_{inc}(Q,t) = I_{inc}^{trans}(Q,t)\cdot I_{inc}^{rot}(Q,t)\cdot I_{inc}^{vib}(Q,t)$$

(5)

Simplifications are possible, depending on the temperature and experimental energy range.

2.4 Theoretical Calculations

The single-chain dynamics in a low molar mass melt can be described by the stochastic Langevin equation in the absence of the hydrodynamic interaction, screened by the surrounding chains. We closely follow the method described in ref. [53], where we theoretically investigated the dynamics of both linear PDMS and of some coarse grained models (freely jointed and freely rotating chains) with different degrees of local stiffness for a comparison. As a result, here we only briefly mention the basic differences due to the constraint of ring closure. We consider

chains comprising N repeat units connected by harmonic springs of length l. Consequently the linear chain and the ring have the same molar mass for a given N, but the number of connecting springs is N-1 and N, respectively. In the freely jointed (FJ) model the spring comprises a few chemical repeat units and corresponds to the statistical segment devoid of any conformational correlation with the adjacent ones. On the other hand, in realistic PDMS the spring encompasses a single chemical repeat unit, or monomer, such that the length l is given by the distance between two sequential units and the conformational correlation is dictated by the preferred rotational states around the individual Si-O bonds within the RIS scheme. The elastic force matrix acting among the directly connected units is obtained as described in ref. [53], and, in the absence of excluded-volume interactions (which are also screened in a melt), only depends on the topologically short-range correlations imposed by the local stiffness in PDMS and by the constraint of ring closure. Diagonalization of the elastic force matrix decouples the dynamics equations and produces both the dynamical normal modes through its eigenvectors, and the (adimensional) intramolecular relaxation rates through the eigenvalues. The elements of the eigenvector matrix, V_{jp}, and the eigenvalues for the linear chain are reported in equations (1) - (4) of ref. [53], while in the case of the ring they are given by

$$V_{jp} = \left(\frac{1}{N}\right)^{1/2} e^{iq_p j} \tag{6}$$

where i is the imaginary unit and the Fourier coordinate q_p is

$$q_p = \frac{2\pi p}{N}, \qquad p = 0, 1, 2, ..., N\text{-}1 \tag{7}$$

The eigenvalues are then given by μ_p/C_p, where

$$\mu_p = 4\sin^2(q_p/2) \tag{8}$$

formally the same as in the linear chain. C_p is the generalized characteristic ratio embodying the conformational features of the chain model. For the FJ chain with no short-range correlation among the bond vectors $C_p \equiv 1$, while in real chains, within the RIS scheme C_p can be written as[65, 66]

$$C_p = \sum_{h=1}^{\nu} \alpha_h \frac{1 - g_h^2}{1 + g_h^2 - 2g_h \cos q_p} \tag{9}$$

Note that with a single term within the sum, and with $\alpha_h \equiv 1$, the above expression applies to a freely-rotating chain model, with $g = -\cos\theta$, θ being the fixed "bond" angle formed by adjacent "bond" vectors. Using the RIS scheme, the $\{\alpha_h, g_h\}$ values for some real polymers, including also PDMS, are reported in ref. [66], with ν in principle equal to three (i.e., the space dimensionality) times the number of rotational energy minima around a single bond. However, in practice, only 4-5 non-vanishing terms are required in the sum of equation (9), provided the chemical repeat unit is effectively treated as a whole. In this case, l is simply equal to the distance between corresponding atoms in adjacent monomers, and it is equal to 2.9 Å as an average value for the Si···Si and O···O separation in PDMS. It should be noted that in a ring polymer, the cyclic symmetry imposes a two-fold multiplicity to the spectrum of the relaxation rate between the modes characterized by the indices p and N-p, as it can be seen through equations (8) and (9). The intramolecular relaxation times τ_p, $p = 1, 2, ..., N-1$ are then given by

$$\tau_p = C_p/\sigma\mu_p \tag{10}$$

where σ^{-1} is the time unit

$$\sigma = 3k_BT/\zeta l^2 \tag{11}$$

ζ being the friction coefficient of the repeat unit.

By assuming a Gaussian distribution of $\boldsymbol{R}_j(t)$ - $\boldsymbol{R}_j(0)$, in view of the stochastic Brownian forces due to the random impulses of the surrounding molecules, the dynamic structure factor for incoherent scattering is obtained from equation (3), as

$$I_{\mathrm{inc}}(Q,t) = \exp\left[-Q^2 Dt\right]\cdot\frac{1}{N}\sum_j \exp\left[-\frac{Q^2}{6}\left\langle r_{jj}^2(t)\right\rangle\right] \tag{12}$$

where we separated the contribution of the zero-th mode with p=0 that yields the diffusion coefficient D, given by the Einstein formula

$$D = k_BT/N\zeta = \sigma l^2/3N \tag{13}$$

from the intramolecular contribution described by the internal modes embodied by the time-dependent mean-square distance of the j-th repeat unit from itself at different times

$$\left\langle r_{jj}^2(t)\right\rangle = \left\langle \left[\boldsymbol{R}_j(t) - \boldsymbol{R}_j(0)\right]^2 \right\rangle - 6Dt \tag{14}$$

irrespective of the position of the centre of mass. Consequently we have (see also ref. [67])

$$\left\langle r_{jj}^2(t)\right\rangle = \frac{2l^2}{N}\sum_{p=1}^{N-1}\frac{C_p}{\mu_p}\left[1-\exp\left(-t/\tau_p\right)\right] \tag{15}$$

Note that in view of the cyclic statistical symmetry of the ring $\left\langle r_{jj}^2(t)\right\rangle$ turns out to be independent of the *j* index of the repeat unit.

The calculated line shapes of $I_{inc}(Q,t)$ for the FJ chain and the PDMS rings, and for the corresponding linear chains (calculated as described in ref. [53]), were then fitted by the KWW stretched exponential function for relatively short times before diffusion of the centre of mass sets in:

$$\frac{I_{inc}(Q,t)}{I_{inc}(Q,0)} = \exp\left(-\left(t/\tau\right)^{\beta}\right) \tag{16}$$

Here, both the characteristic time τ and the β exponent (<1) are assumed to depend both on Q and on N in the theoretical approach. The calculations were carried out for linear chains and rings with a number of repeat units, $10 \le N \le 200$ (beads for the freely jointed model and monomers for real PDMS), in the range of the experimental samples choosing a Q range of $0.2 \le Q\cdot l \le 1.0$. From the non-linear fit of the calculated line shape using the stretched exponential of eq. (16), the correlation coefficient R turned out to be larger than 0.9999 for the FJ chain and 0.9997 for PDMS, while the mean-square residuals χ^2, normalised by the number of degrees of freedom, was smaller than $2.5\cdot10^{-6}$ for the FJ chain and $3.5\cdot10^{-5}$ for PDMS.

3. RESULTS

3.1 Analysis of low temperature data of cyclic PDMS

In our previous studies[55-57], we have shown that the QENS data of PDMS melts are described by a model that consists of two dynamic contributions: methyl group rotation and segmental motion. To test whether changes to methyl group dynamics needed to be accounted for in cyclic polymers, we carried out a series of measurements on a cyclic sample with M_w = 2675 g mol^{-1}

(C2700) in the temperature range 158 K to 208 K. Although this corresponds to temperatures above T_g, segmental dynamics are slower than the temporal range probed by the IRIS and OSIRIS instruments and thus do not contribute to quasielastic broadening[55-57]. Bearing this in mind, the incoherent dynamic structure factor can be expressed in terms of the rotational scattering law of the side groups:

$$S_{inc}(Q,\omega) = DWF\ \left[A_o(Q)\delta(\omega) + S_{inc}^{qel}(Q,\omega)\right] \tag{17}$$

where DWF is the Debye-Waller factor[68] and $A_o(Q)$ is the elastic incoherent structure factor (EISF), which represents the space-Fourier transform of the final distribution of the scattering centers, averaged over all possible initial positions. For a three-fold jump rotation, $A_o(Q)$ is given by:

$$A_o(Q) = \frac{1}{3}\left(1 + 2\ j_o\left(\sqrt{3}Q \cdot r\right)\right) \tag{18}$$

$j_o(x)$ being a zero-order spherical Bessel function and r the distance between the moving protons and the rotation axis. Within the rotational rate distribution model, RRDM, the quasi-elastic component is described by a log-Gaussian distribution of Lorentzian lines $L_i(\omega)$[69, 70]:

$$S_{inc}^{qel}(Q,\omega) = \left[1 - A_o(Q)\right] \sum g_i L_i(\omega) \tag{19}$$

where $L_i(\omega) = \frac{1}{\pi} \cdot \frac{\Gamma_i}{\Gamma_i^2 + \omega^2}$. The parameter g_i represents the weight of each Lorentzian line:

$$g\left(\ln \Gamma_i\right) = \frac{1}{\left(2\pi\sigma_\Gamma{}^2\right)^{0.5}} \exp\left[\frac{-\left(\ln \Gamma_i - \ln \Gamma_o\right)^2}{2\sigma_\Gamma{}^2}\right] \tag{20}$$

σ_Γ being the width of the distribution of rotational frequencies and Γ_o the most probable width of the quasi-elastic component. For side group motion, the temperature dependence of the quasi-elastic component is described by the Arrhenius equation:

$$\Gamma_o(T) = \Gamma_\infty \exp\left[-\frac{E_a}{RT}\right] \tag{21}$$

where E_a is the activation energy barrier for rotation, R the gas constant and Γ_∞ the attempt to escape frequency or jumping frequency at infinite temperature.

The above equations are used to fit the experimental data, after convolution with the instrumental resolution, $R(Q,\omega)$ and addition of a flat background $B(Q)$:

$$S(Q,\omega) = F(Q)\cdot\left[A_o(Q)\,\delta(\omega) + \left(\left(1-A_o(Q)\right)\sum_{i=1}^{N} g_i L_i(\omega)\right)\right] \otimes R(Q,\omega) + B(Q) \qquad (22)$$

where the term $F(Q)$ is a temperature and Q dependent scaling factor. The flat background *B(Q)* represents any fast process outside time window of instrument.

For the purpose of the present study, we note that the low temperature data of cyclic PDMS (C2755) are well represented by equation (22), using parameters reported by us for linear PDMS[55, 56] (Γ_∞ = 0.63 $\pm$ 0.06 meV, E_a = 4.5 $\pm$ 0.5 kJ mol^{-1} and the width of the distribution of activation energies, σ_E = 1.1 $\pm$ 0.1 kJ mol^{-1}) and fixed *EISF* values for the three-fold methyl group dynamics. The agreement between calculated and experimental values is shown in Figure 1 for Q = 1.31 Å^{-1} at 158 K, 183 K and 208 K.

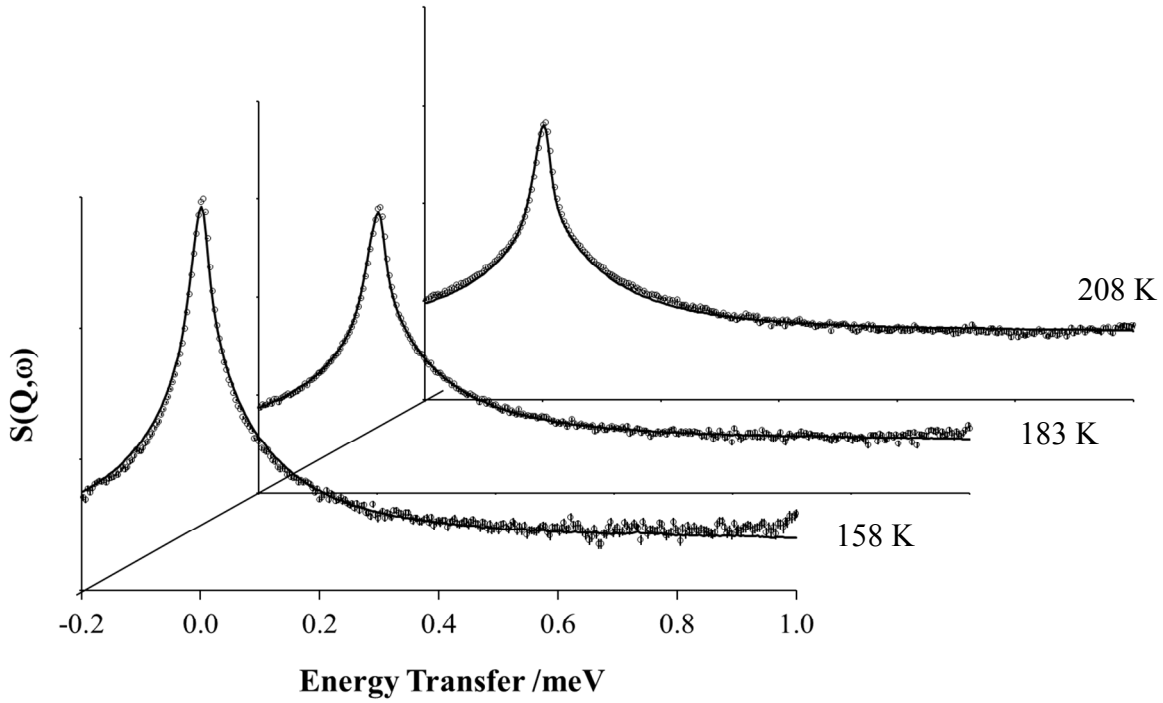

Figure 1 – QENS spectra of cyclic PDMS (C2755) at 158 K, 183 K, 208 K (from front to back) and Q = 1.31 Å^{-1}. Symbols represent experimental data and lines are calculated S(Q,ω) curves using equations 18 to 22 with Γ_∞ = 0.635 meV, σ_E = 1.1 kJ mol^{-1} and E_a = 4.5 kJ mol^{-1} and fixed EISF values. The only adjustable parameters are F(Q) and B(Q).

Perhaps more surprisingly, good agreement between calculated $S(Q,\omega)$ values and experimental data is also found for very small cyclics. As shown in Figure 2 for C445 for T = 240 K, calculations closely match the Q dependence of the quasi-elastic broadening. However, deviations are observed at the lowest and highest Q values. Fits using equations (18) to (22) are shown in the Supplementary Information (SI). We note that the fitting parameters and the corresponding values of Γ_∞,, σ_E and E_a (see SI) are sufficiently close to those reported by us previously[55] and so these will be used again here to fit the high temperature data.

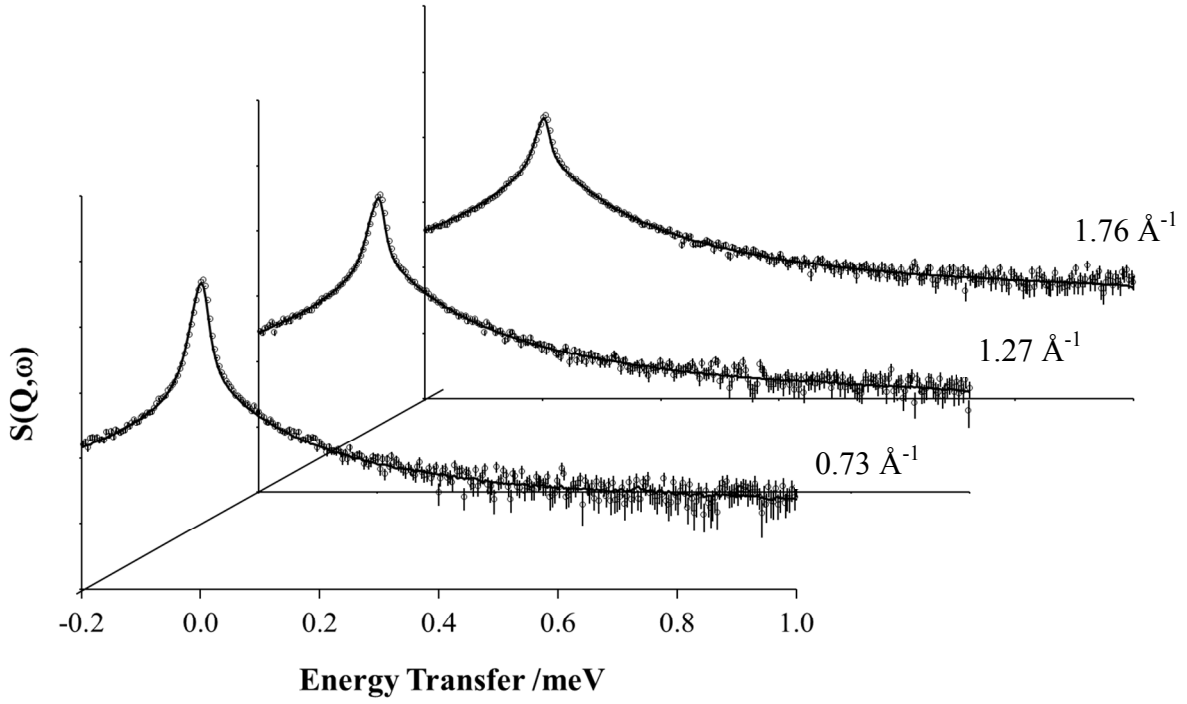

Figure 2 – QENS spectra of cyclic PDMS (C445) at 240 K and Q = 0.73, 1.27 and 1.76 Å^{-1} (from front to back). Symbols represent experimental data and lines are calculated S(Q,ω) curves using equations 18 to 22 with Γ_∞ = 0.635 meV, σ_E = 1.1 kJ mol^{-1} and E_a = 4.5 kJ mol^{-1} and fixed EISF values. The only adjustable parameters are F(Q) and B(Q) (equation 22).

3.2 Theoretical results

As previously pointed out and also noted in ref. [53] for linear chains, the fit of the calculated $I_{inc}(Q,t)$ using the KWW function was in all cases excellent. The fitted β exponents are reported in Figure 3*a* as a function of $Q \cdot l$ for the various cases. As a general trend, we find that: *i*) β increases with the local stiffness of the chain; *ii*) β decreases somewhat with an increasing molar mass in particular at small Q values; *iii*) while β is slightly larger for the linear chain than for the ring at very small molar mass, this difference becomes quickly negligible with an increasing molecular length; tending to a value close to about 0.65 as found in ref. [53] for linear chains only.

As already done in ref. [53], the characteristic time τ depends on Q through the power law

$$\tau = \tau_0 \cdot Q^{-\alpha} \tag{23}$$

Also in this case, eq. (23) describes very accurately the Q-dependence of τ, as shown by the correlation coefficient larger than 0.9990 for the FJ chain and 0.9986 for PDMS obtained by the fit of τ vs. Q.

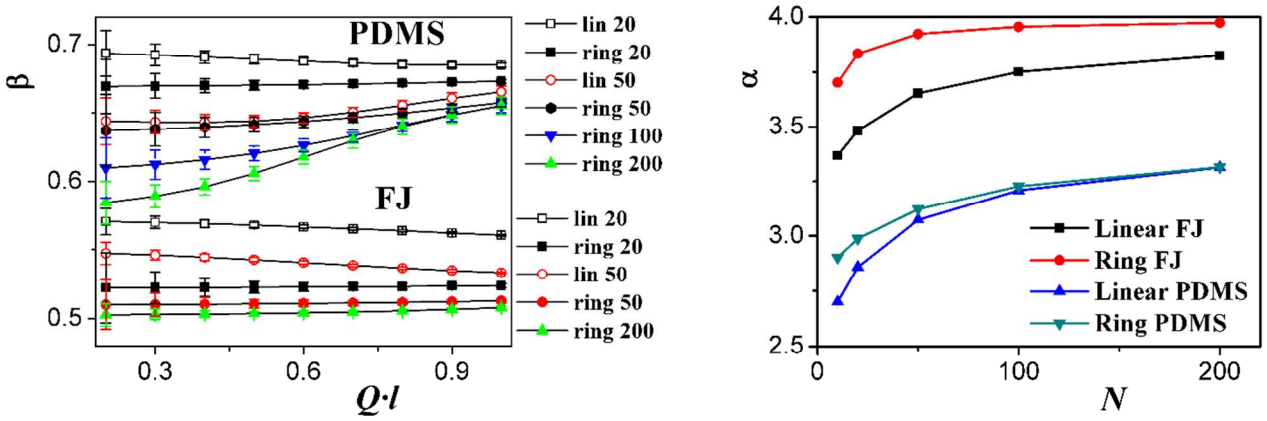

Figure 3 - a) The β exponent plotted vs. Q·l for the FJ chain model and for PDMS with the topology and the selected N values shown in the legend. b) The α exponent plotted as a function of N for the FJ chain model and for PDMS with the topology shown in the legend. In both panels, the error bars obtained in the fitting procedure are shown, although in most cases they are smaller than the symbol size.

The fitted values of α plotted as a function of *N* are shown in Figure 3*b*. The α exponent is larger for the FJ chain than for the more realistic PDMS chain having a local stiffness, and it is larger for the ring than for the linear chain. While this difference is very small for PDMS, unlike for the FJ chain, in both cases α increases monotonically with *N*, hence with molar mass, to an asymptotic constant value very close to 4 for the latter and most likely independent of the molecular topology. On the other hand, the asymptotic value for PDMS is smaller, tending to a value close to 3.4 as obtained for much larger linear chains in ref. [53].

The τ_0 values obtained from equation (23) are plotted as a function of *N* in Figure 4. The characteristic time shows an interesting difference between the linear chains and the rings at relatively small molar mass, whereas the asymptotic value for very large *N* is independent of molecular topology, as could be expected. In particular, the ring shows a larger τ_0 both in the FJ chain model and in PDMS. However, this difference becomes negligible for very large *N*, hence for very large molar masses, so that asymptotically the same τ_0 is achieved for both topologies. Moreover, the results obtained for realistic PDMS chains, accounting for the (albeit limited) conformational rigidity related with the preferred rotational states around the Si-O, show a further slight increase of τ_0 in small rings with N ≈ 50 compared to the linear chains, thus producing a shallow maximum in Figure 4*b*. A discussion of the physical origin of these theoretical results is deferred to the later discussion in comparison with the experimental results.

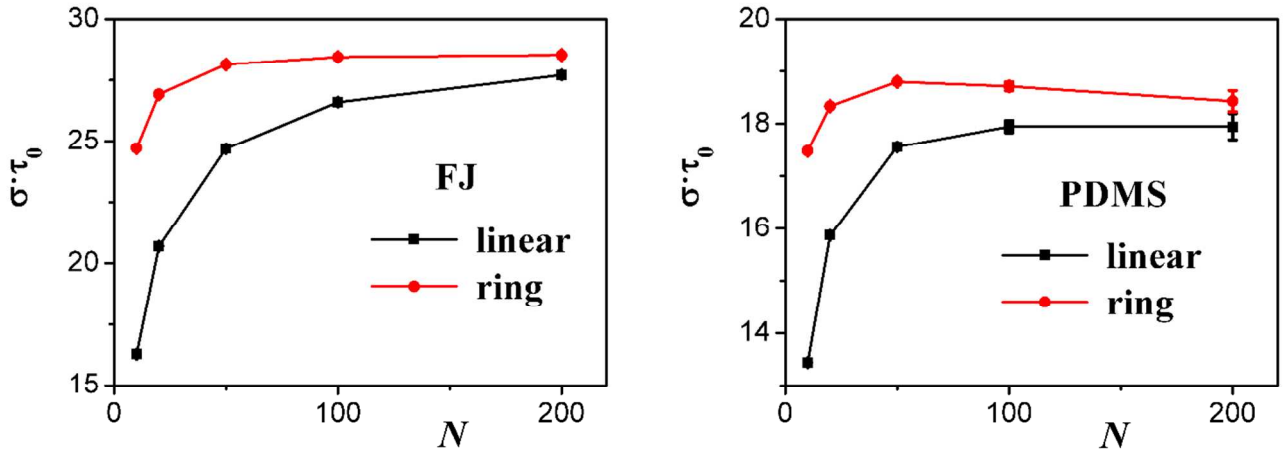

Figure 4 - The effective characteristic time τ_0 in σ^{-1} units (see eq. (11)) plotted as a function of N for a) the FJ chain model and b) PDMS. In both panels, the error bars obtained in the fitting procedure are shown, even though they are smaller than the symbol size.

3.2 Analysis of QENS data at constant T

The molecular weight of the chain dynamics shows features that are consistent with the theoretical calculations. As shown in Figure 5 and Table 1, QENS measurements were carried out on a series of linear and cyclic PDMS samples at approximately 110 degrees above the samples' T_g. For all samples, full broadening of the elastic line is observed but changes with molecular weight appear to be more pronounced for the linear than for cyclic PDMS.

A qualitative indication of the dynamic changes due to topology is given in Figure 6 where we compare, at the same temperature (280 K) a cyclic (C1200) and a linear PDMS (L1400) sample with similar average number of monomers (N_n =16.4 and N_n =19.3, respectively).

To extract quantitative information on the molecular weight dependence of the segmental relaxation, we follow our previous QENS analysis of high molecular weight linear PDMS.[55, 56] In that work, we showed that, for PDMS, CH_3 rotations make a non-negligible contribution to the QE broadening (at least within the timescale of the IRIS spectrometer). Thus, the dynamic incoherent structure factor is described by the convolution of two functions, one representing the local segmental relaxation, and the other one the rotational motion of the CH_3 groups.

As discussed in references [55] and [56], the segmental motion can be expressed by the Fourier transform of the KWW function or equivalent expressions such as the Havriliak-Negami equation[71, 72]. The $S(Q,\omega)$ contribution from methyl group rotations is obtained by extrapolation of data acquired at T < T_m to the desired temperature. This procedure assumes no substantial change, i.e. similar energy landscape[73], for the methyl group motion across T_g and T_m. Hence, the model function is given by:

$$S(Q,\omega) = F(Q)\cdot\left[A_o(Q)\delta(\omega) + \left(\left(1-A_o(Q)\right)\sum_{i=1}^{N} g_i L_i(\omega)\right)\right] \otimes S_{KWW}(Q,\omega) \otimes R(Q,\omega) + B(Q) \quad (24)$$

where $S_{KWW}(Q,\omega)$ is the Fourier integral of the KWW function (equation 16).

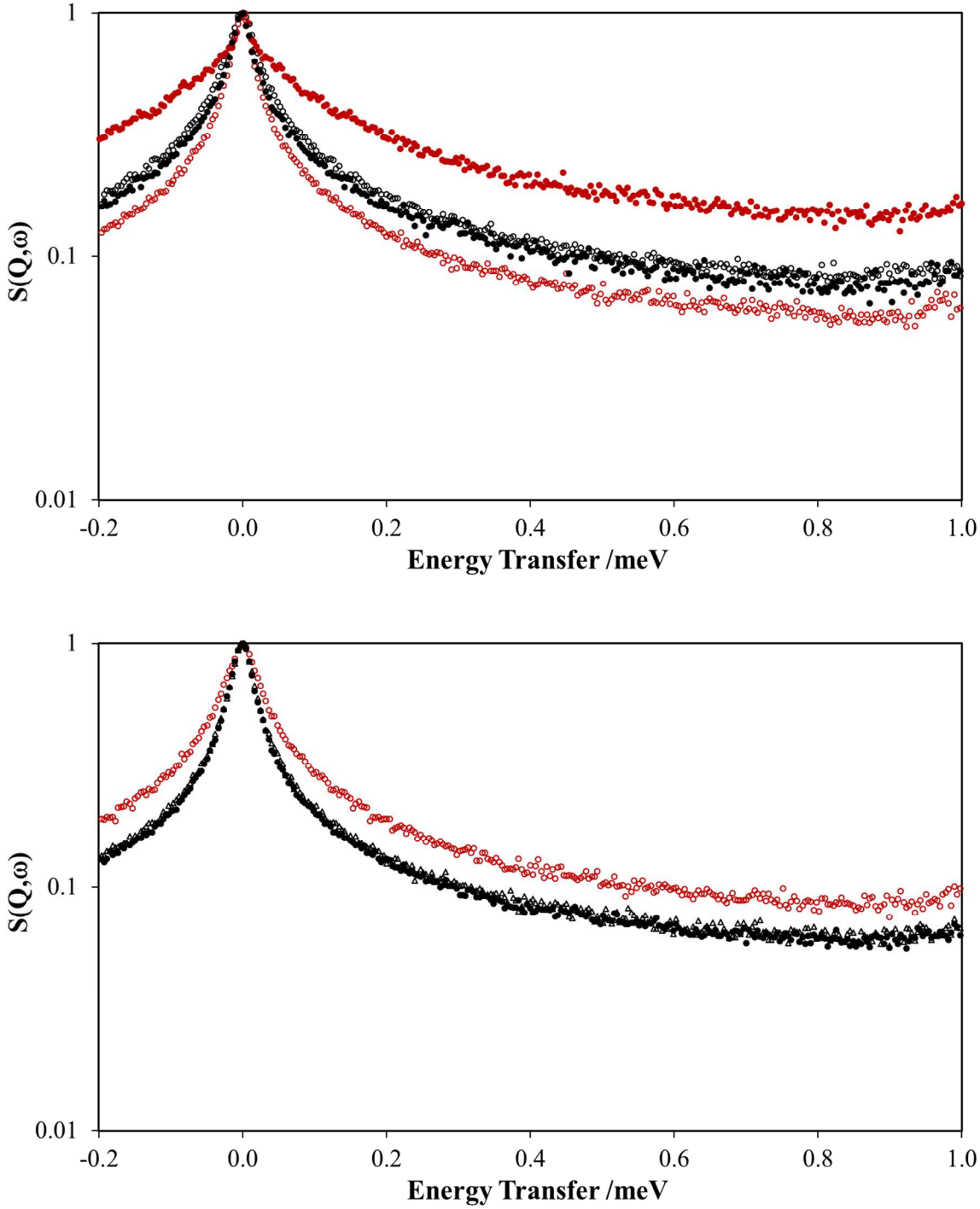

Figure 5 - QENS spectra at Q = 1.45 Å^{-1} of (a) L237, L2000, L3800 and L9430 (from top to bottom) and (b) C370 (○), C1200 (Δ) and C2700 (●) at ca. 110 degrees above the sample's T_g.

(Note: the small upturn for energy transfer values above ca. 0.9 meV is a result of data reduction artefact due to normalization.)

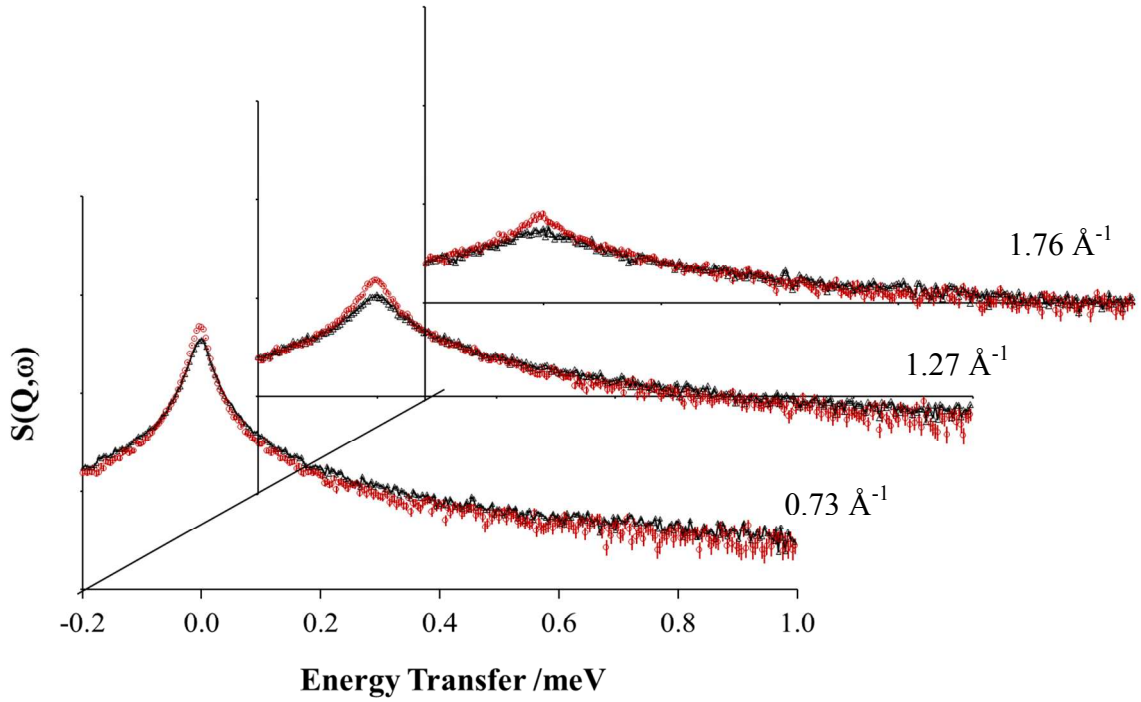

Figure 6 – Comparison between QENS spectra of linear and cyclic polymers with similar number of monomers at 280 K and Q = 0.73, 1.27 and 1.76 Å^{-1}: (○) C1200 and (Δ) L1400. For clarity, error bars are only shown for the cyclic data.

All experimental data collected at temperatures above T_m are well described by equation (24), irrespective of molecular weight and topology. The quality of fits is shown in Figures 7 and 8 for linear (L1400) and cyclic (C2700) PDMS samples of intermediate molecular weights.

At first, the $S(Q,\omega)$ data were fitted at each Q value to determine the Q dependence of the KWW parameters i.e. the stretched exponent β and the characteristic time τ. As shown in Figure 9, even for very small chains, a unique Q dependence can be identified for Q values above 0.5 Å^{-1}. In this Q range, β values were found to be Q independent (Figure 10). This finding is consistent with our earlier study of linear high molecular weight PDMS[55, 56].

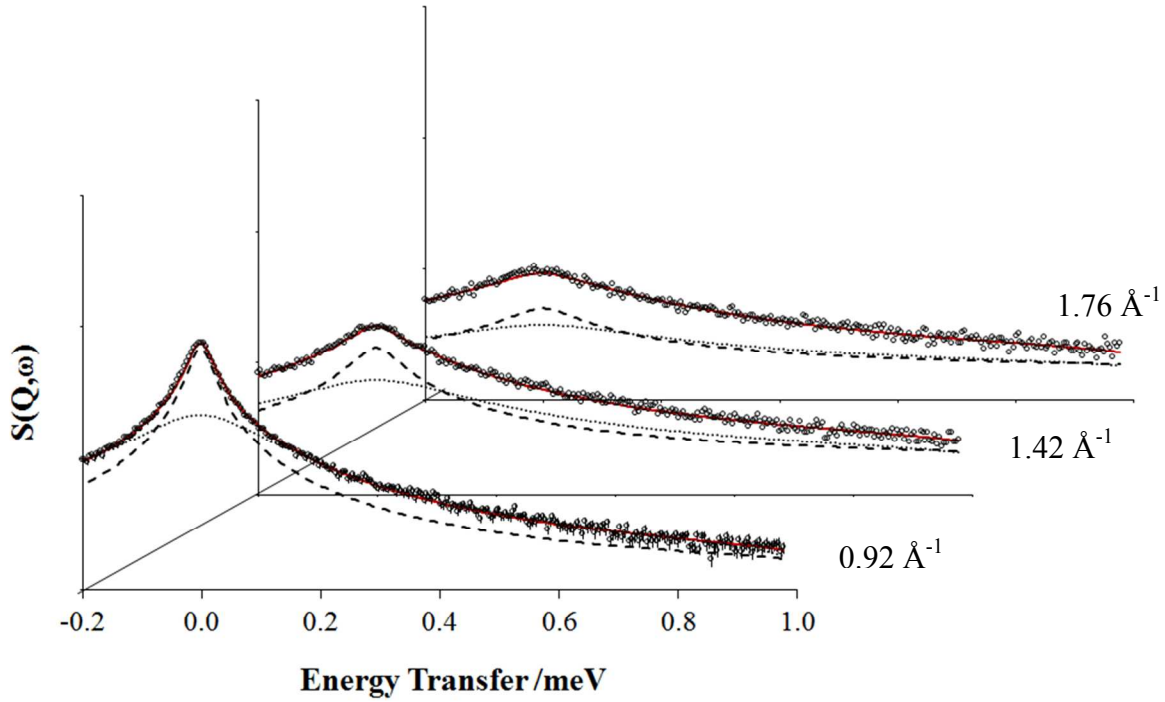

Figure 7 – QENS spectra of L1400 at 298 K and Q equal to 0.92, 1.42 and 1.76 Å^{-1} (from front to back). Symbols represent experimental data while full lines are fits using equation (24). The dashed and dotted lines represent the two dynamic contributions: (a) segmental dynamics (dashed) and methyl rotations (dotted). For clarity, error bars are only shown for one set of data (Q = 0.92 Å^{-1}).

To account for differences in the distribution of relaxation times, effective times, τ_{eff}, were calculated using the relationship:

$$\tau_{eff} = \tau \frac{\Gamma\left(\frac{1}{\beta}\right)}{\beta} \qquad (25)$$

Values of τ_{eff} are also plotted in Figure 9 and compared to the trend obtained by fitting simultaneously at all Qs using equations (23), (24) and (25).

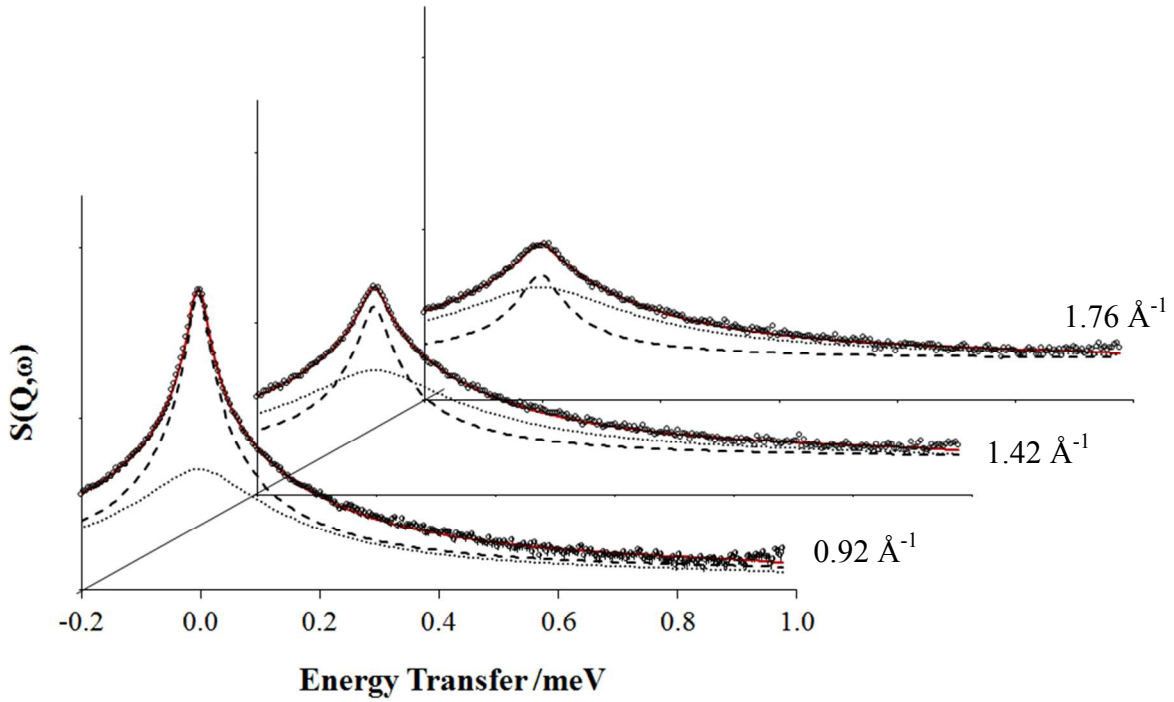

Figure 8 – QENS spectra of C2700 at 283 K and Q equal to 0.92, 1.42 and 1.76 Å^{-1} (from front to back). Symbols represent experimental data while full lines are fits using equation (24). The dashed and dotted lines represent the two dynamic contributions: (a) segmental dynamics (dashed) and methyl rotations (dotted). For clarity, error bars are only shown for one set of data (Q = 0.92 Å^{-1}).

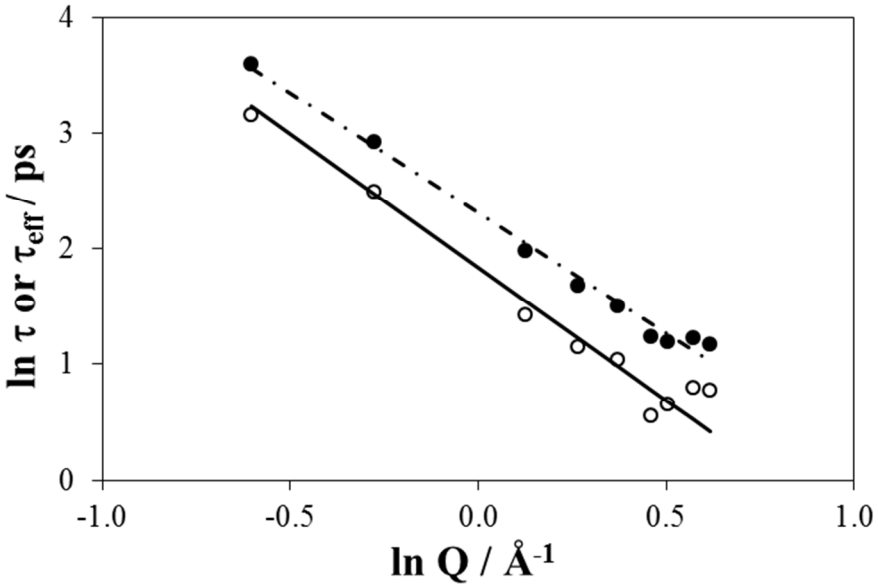

Figure 9 – Q dependence of the characteristic time, τ (○) and τ_{eff} (●) (equation 25) as obtained from fitting data of L237 at 235K using equation (24). The lines represents values obtained by simultaneous fits using equations (23)to (25).

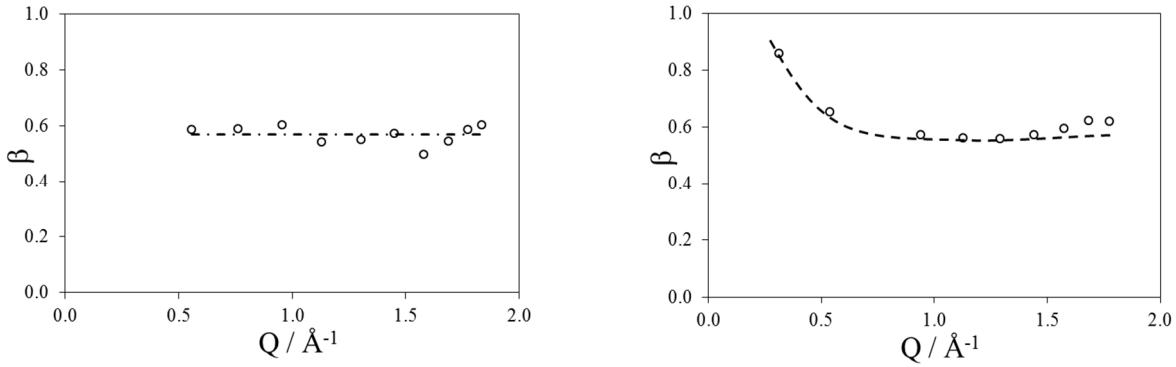

Figure 10 – Q dependence of the β parameter as obtained from fitting data of (a) L237 at 235K (IRIS data) and (b) L550 at 235 K using equation (24). The lines represent a guide to the eye.

However, analysis of OSIRIS data for L550 revealed a sharp increase in β values towards unity ($\beta \sim 0.8$) at the lowest Q (Figure 9). This is attributed to contributions from center of mass diffusion which, at small Q values, is expected for small molecules. Diffusion of the whole molecule can be described by a single exponential function corresponding to a Lorentzian line in the frequency domain. In our analysis, this corresponds to a stretched exponent $\beta = 1$.

The OSIRIS data of L550 (Figure 10b) confirm that, at Q > 0.5 $Å^{-1}$, β is, within experimental error, independent of the momentum transfer, Q.

The molecular weight dependence of the stretched exponent β (Figure 11) suggests that β decreases with increasing molar mass for both linear chains and cyclics, reaching a constant value at high M_n which is equal to 0.56 and 0.52 for linear and cyclic polymers, respectively. Our experimental data lend support to the predicted trend (Figure 3) that β increases with decreasing molar mass and it is lower for cyclics compared to linear chains of the same molecular weight. This effect may be attributed to conformational restrictions in cyclic compared to linear PDMS. We note, however, that changes in experimental β values are relatively small compared to those predicted by theory (Figure 3).

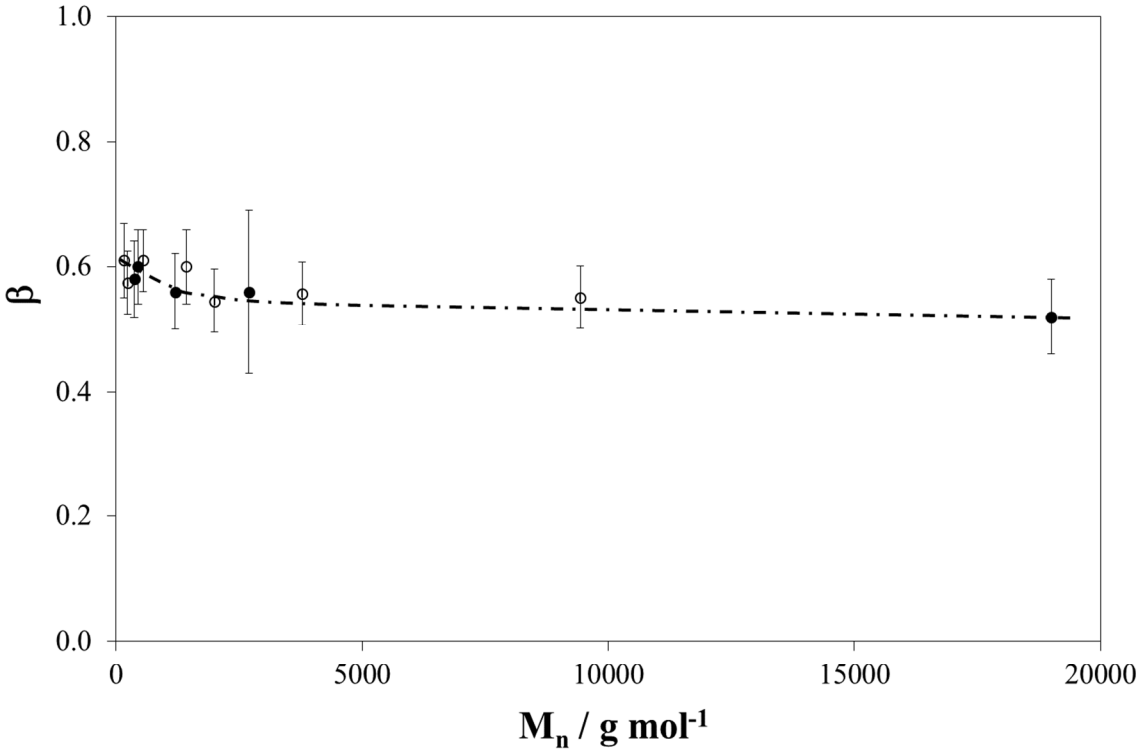

Figure 11 – Molar mass dependence of the stretched exponent as obtained from fits of the S(Q,ω) data at ca. 110 degrees above T_g for: (○) linear PDMS and (●) cyclic siloxanes. The line is a guide to the eye.

Very few studies of local chain dynamics have been published and the results are somewhat contradictory. For example, dielectric spectroscopy (DS) measurements carried out by Krist *et al*. found $\beta = 0.485$ for both linear and cyclic polymers suggesting no change in the distribution of relaxation times with topology.[58] Similar work by Goodwin *et al*. reported a slightly lower β average value ($\beta = 0.48$) for linear compared to cyclic ($\beta = 0.53$) PDMS[61]. This result was taken as an indication that -relaxation is more cooperative in linear PDMS.

Here we note that, although average β values are lower for cyclics, changes are within experimental error. (Figure 11).

To be able to make quantitative comparison between the timescales of the segmental relaxation in PDMS samples, we calculated effective times, τ_{eff}, from τ at $Q = 1$ Å^{-1}, i.e. τ_o, using equation (25). τ_{eff} values are plotted in Figures 12 and 13 as a function of molecular weight, for both linear and cyclic PDMS.

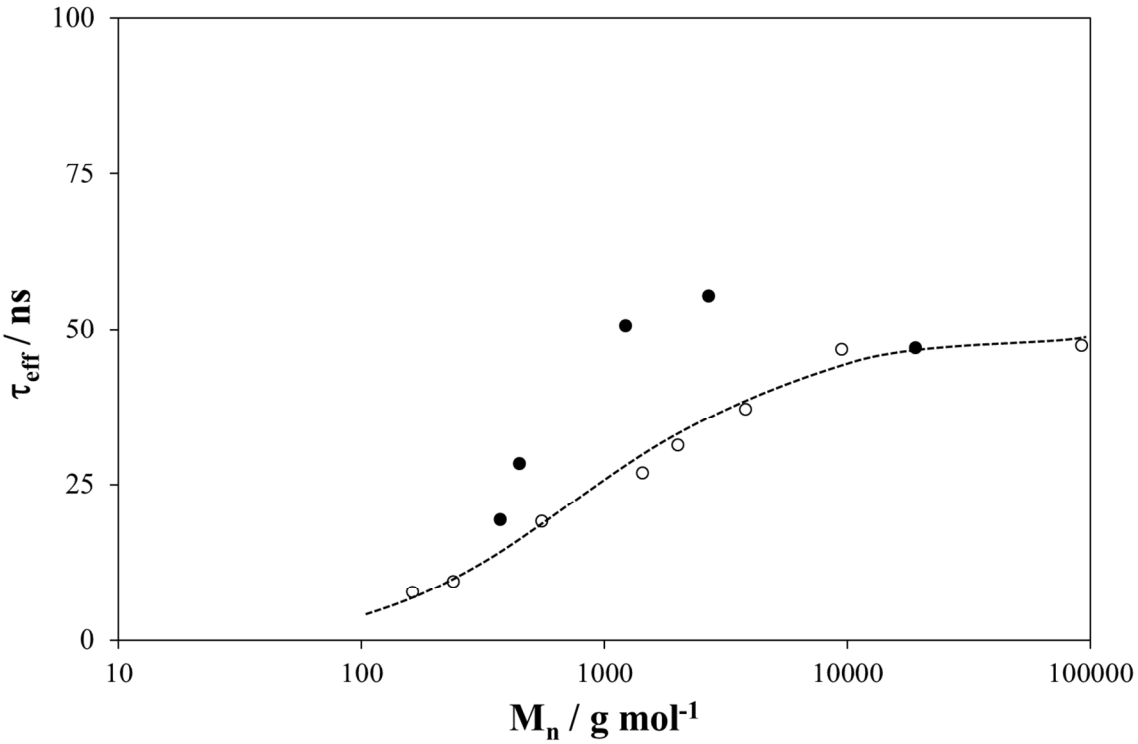

Figure 12 – Molar mass dependence of τ_{eff} for linear (○) *and cyclic* (●) *PDMS at ca. 110 degrees above the corresponding glass transition. The dotted line is a guide to the eye.*

Values of τ_{eff} plotted in Figure 12 refer either to measurements carried out at T_g + 110°C or values scaled to this temperature using experimentally determined activation energies (see following section). The τ_{eff} value reported by us previously for a linear PDMS sample with M_w = 91,700 g mol^{-1} (=47.5 ps), also shown in Figure 12, compares well with the value for the highest M_n sample investigated here.

As shown in Figure 12, differences in the glass transition temperature of the samples are not sufficient to account for the molar mass dependence of the relaxation times. For linear siloxanes, τ_{eff} increases, i.e. molecular motion slows down, with increasing molar mass. A similar trend has been reported for polyisobutylene (PIB) by Frick *et al*.[74]. These authors noted that T_g differences and contributions from centre of mass diffusions at low molar mass could not fully account for the observed dynamic changes with chain length. It was suggested that the discrepancy was due to faster motion of near chain-end groups. This idea was supported by experiments in the glassy state.

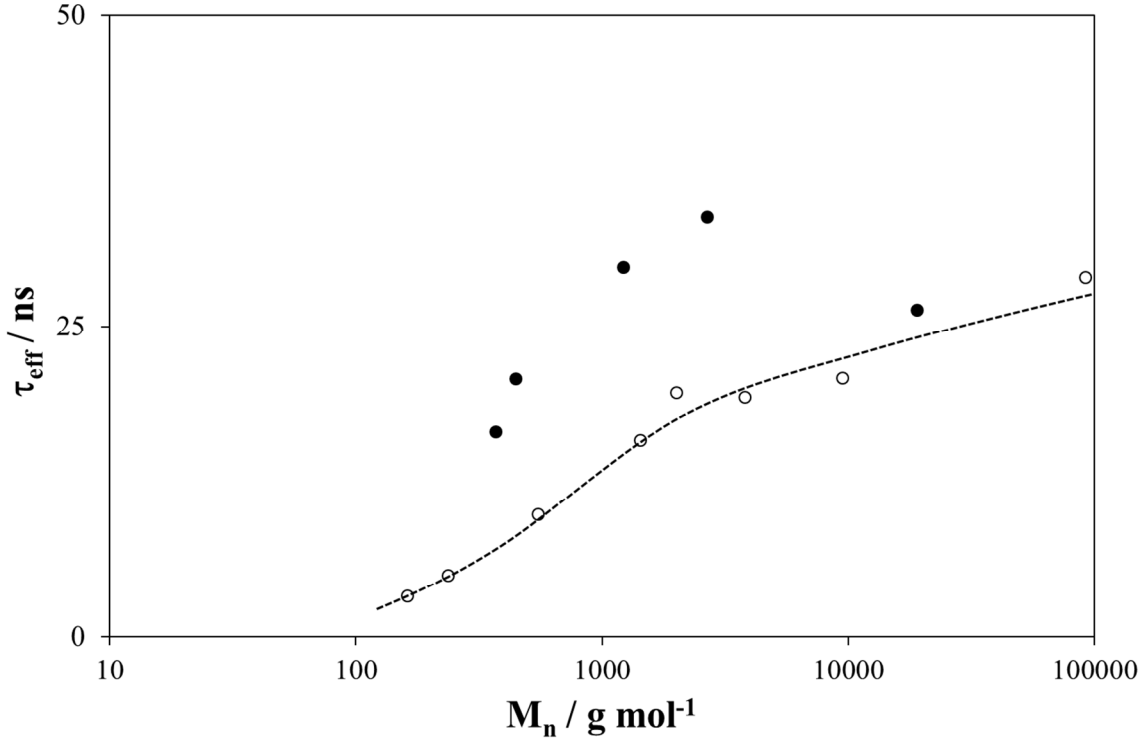

Figure 13 – Molar mass dependence of τ_{eff} for linear (○) *and cyclic* (●) *PDMS at 280K. The dotted line is a guide to the eye.*

The QENS data reported here were collected at Q values above 0.5 $Å^{-1}$ and, as discussed earlier, little or no contribution from centre-of mass diffusion are expected even for small chains. Therefore, having accounted for T_g changes, the observed trend supports the idea that mobile chain ends are responsible, at low M_n, for the faster dynamics.

The closed structure of rings implies no contribution from fast chain ends. Therefore, one might expect that, once T_g changes are accounted for, relaxation times are independent of molar mass. This is not the case for our data (Figure 12) and although τ_{eff} values for cyclic PDMS are higher compared to those of linear samples, there is a clear M_n dependence. In particular, τ_{eff} increases with increasing degree of polymerisation, reaches a maximum and, for M_n=19000 g mol^{-1} approaches values characteristic of linear chains. On the other hand, this trend is consistent with theoretical predictions in terms of τ_o (Eq. (23) and Figure 4). To understand this behaviour, it should be noted that the local segmental relaxation proceeds through the conformational rearrangements around the chemical bonds of the main chain. Thus, the ring shows a lengthier relaxation due to the topological constraint imposed by the ring closure: this feature slows down the local dynamics compared to the linear chain whose dynamics is faster thanks to its free ends. This effect is already evident in the FJ chains devoid of any local rigidity and corresponding to the familiar bead-and-spring chain. Moreover, it is further enhanced in PDMS by the additional constraint of the (limited) conformational rigidity related with the preferred rotational states around the Si-O bonds, as anticipated, producing a shallow maximum (Figure 4b) fully consistent with the experimental results of Figure 12.

Figure 12 suggests that the dynamics of small rings is not that different from motion of very short chains. However, one should bear in mind that τ_{eff} values reported in Figure 12 were obtained in some cases at considerably different temperatures. For example, there is a 40 degrees difference between τ_{eff} of C370, measured at 275 K, and the corresponding value for L237, measured at 235K. To appreciate how τ_{eff} changes with molar mass and topology, we have reported in Figure 13 values at a common temperature of 280 K. Greater changes with topology can be observed in this case since differences in T_g are not accounted for.

Finally, we note that the exponent, α, obtained by assuming a power law dependence of the characteristic time (equation 23), was found to vary in the range 1.86 ± 0.05 for L162 to 2.5 ± 0.1 for L1400. These values are lower than those obtained by us for linear high molecular weight

PDMS (α ca. 2.3)[53, 55, 56], suggesting a very weak, if any, molecular weight dependence. We note that larger values are obtained if methyl group rotations are not accounted for, with α in the range 3.0 to 3.3 for high molecular weight PDMS, depending on temperature. It is also interesting to point out that the values of α in the latter range nicely agree with the theoretical ones reported for PDMS in Figure 3b where the methyl group rotations is also ignored. Similar observations were made by Frick *et al.*[74] who studied the molecular weight and Q dependence of the relaxation times of PIB at 368 K from 0.2 to 1.9 Å^{-1}. In that work, a change from $\tau \propto Q^{-2/\beta}$ at low Q to $\tau \propto Q^{-2}$ at high Q was observed for samples with M_w ranging from 680 to 73000 g mol^{-1}. Our data samples relatively high Q values and such cross-over is not evident.

For cyclic PDMS similar α values were obtained within a relatively narrow range from 2.1 to 2.8, depending on molar mass and temperature (the error in all cases is estimated to be ca. 0.2).

3.3 Temperature dependence of segmental motion for linear and cyclic PDMS

As briefly mentioned in the previous section, in addition to measurements carried out at equal distance from T_g, QENS data were also collected, for selected linear and cyclic samples at a series of temperatures above T_m. To simplify data analysis, the $S(Q,\omega)$ spectra were fitted simultaneously using a constant β and $\tau = \tau_o Q^{-\alpha}$. Example of fits are shown in Figure 14 for C2755 at T= 258, 283 and 308 K.

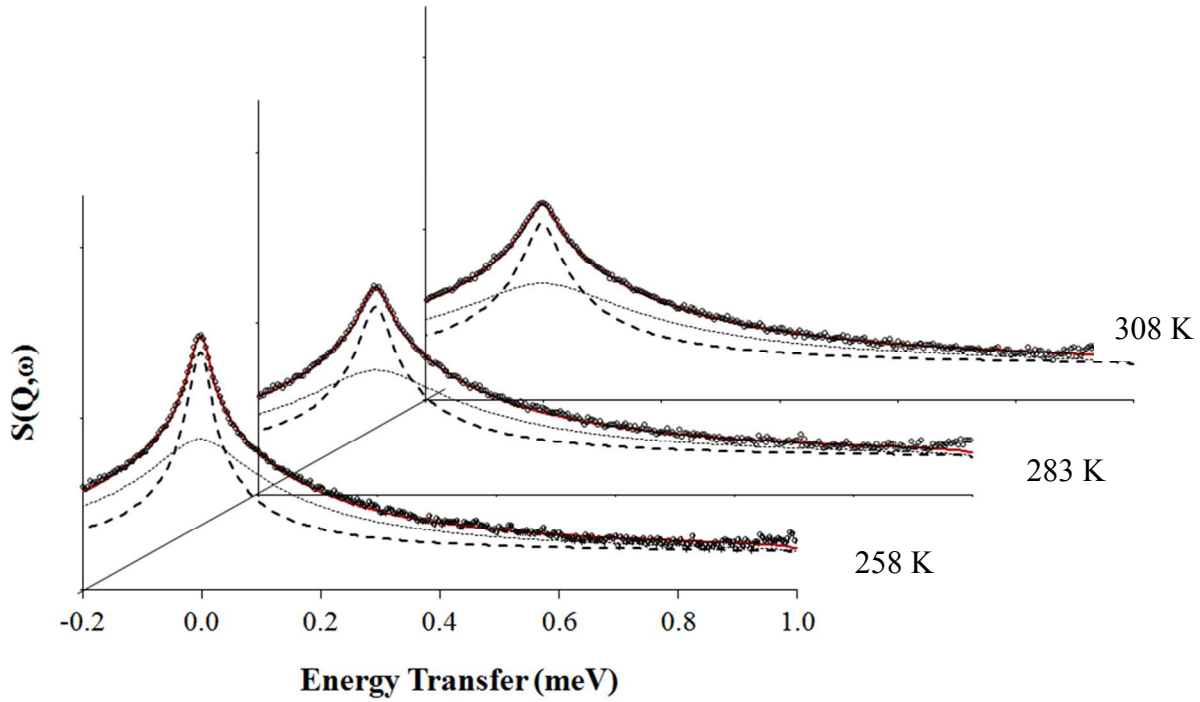

Figure 14 – QENS spectra of C2755 at Q = 1.45 Å^{-1} and three temperatures above T_g : 258, 283 and 308 K (from front to back). Symbols represent experimental data while full lines are fits using equation (24). The dashed and dotted lines represent the two dynamic contributions: (a) segmental dynamics (dashed) and methyl rotations (dotted).

The temperature and molar mass dependence of τ_{eff} for all samples investigated is shown in Figure 15. As shown by us elsewhere, for PDMS samples at T above T_m, both viscosity and relaxation times follow an Arrhenius temperature dependence[53, 55, 56]:

$$\tau_{eff} = \tau_\infty e^{E_a / RT} \quad (26)$$

where E_a is the activation energy, R the gas constant and τ_∞ is the relaxation time at infinite temperature.

As shown in Figure 15, equation (26) applies to all QENS data, irrespective of molar mass and topology. The variations in τ_{eff} values mimic the trend reported earlier (Figures 12 and 13). For linear chains relaxation times are strongly dependent upon molar mass, increasing as M_n increases. However, for cyclic PDMS, τ_{eff} increases from C370 to C2700 and consistently lower values are obtained for C19000, at all temperatures (even below those of the linear samples).

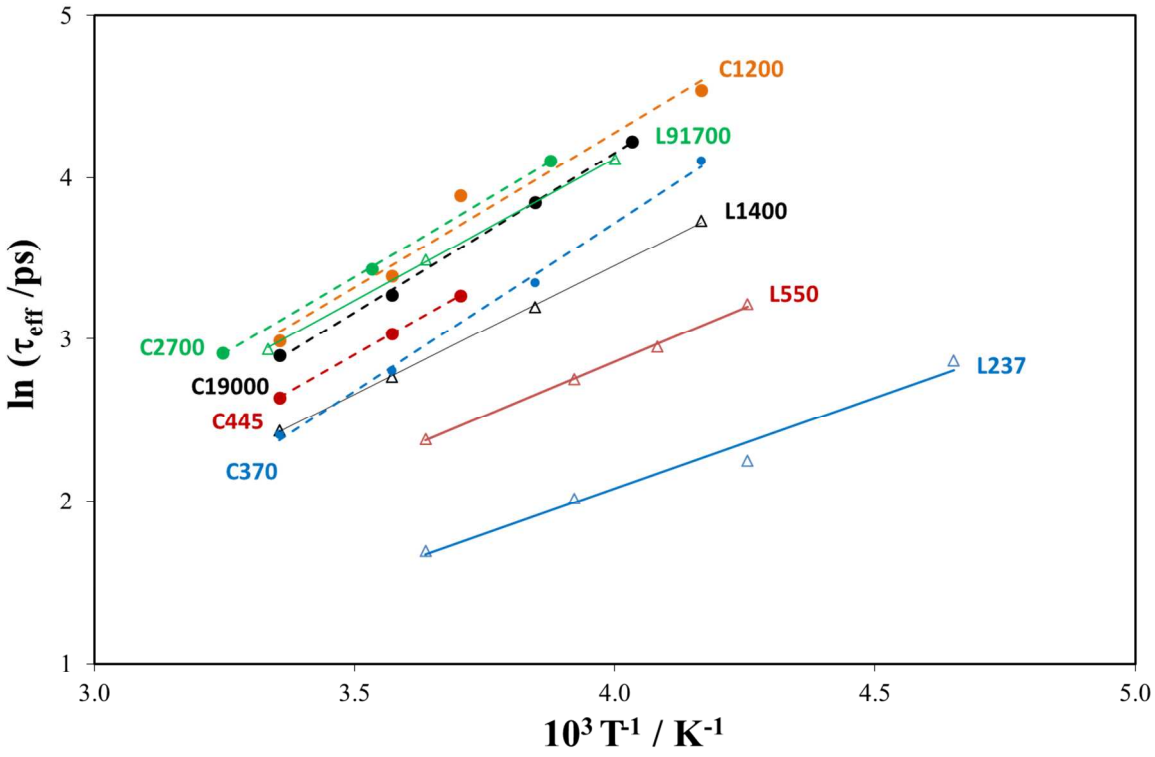

Figure 15 – Temperature dependence of τ_{eff} for linear and cyclic PDMS samples. The lines are fits to the experimental points using the Arrhenius equation.

Activation energies can be calculated from the slope of ln τ_{eff} versus 1/T (Figure 15). E_a values are plotted in Figure 16 for both cyclic and linear PDMS, and compare to literature data from bulk viscosity measurements of Dodgson *et al.*[10-12].

At first inspection, agreement with viscosity measurements appears to be closer for linear than for cyclic PDMS. For linear chains, E_a increases with increasing molar mass from 9.3 $\pm$ 1.0 kJ mol^{-1} for L237 to 14.6 $\pm$ 0.3 kJ mol^{-1}, the value reported by us for L91700 in reference 49.

Viscosity data of Dodgson *et al.*[10-12] show that, for cyclic PDMS, activation energies decrease with increasing molar mass, contrary to the decrease observed for linear PDMS. For both cyclic and linear PDMS a constant value is reached at high molar mass which is equal to ~14.8 kJ mol^{-1} for the linear samples. For cyclics a higher value (~15.5 kJ mol^{-1}) was obtained.

Although our data provide clear evidence that activation energies are higher for cyclics compared to linear chains, there is no unambiguous trend with molar mass. Values range from

17.4 ± 0.7 kJ mol^{-1} for C370 to 16.2 ± 0.9 kJ mol^{-1} for C19000. The relatively high value recorded for C370 is not unexpected based on QENS measurements of small rings carried out several years ago by us where a value of 21 kJ mol^{-1} was reported for hexamethylcyclotrisiloxane (M_n = 222.5 g mol^{-1}). However, the reason why there is such a discrepancy between E_a values of C370 and C445 (15.2 ± 0.1 kJ mol^{-1}) is at present unclear.

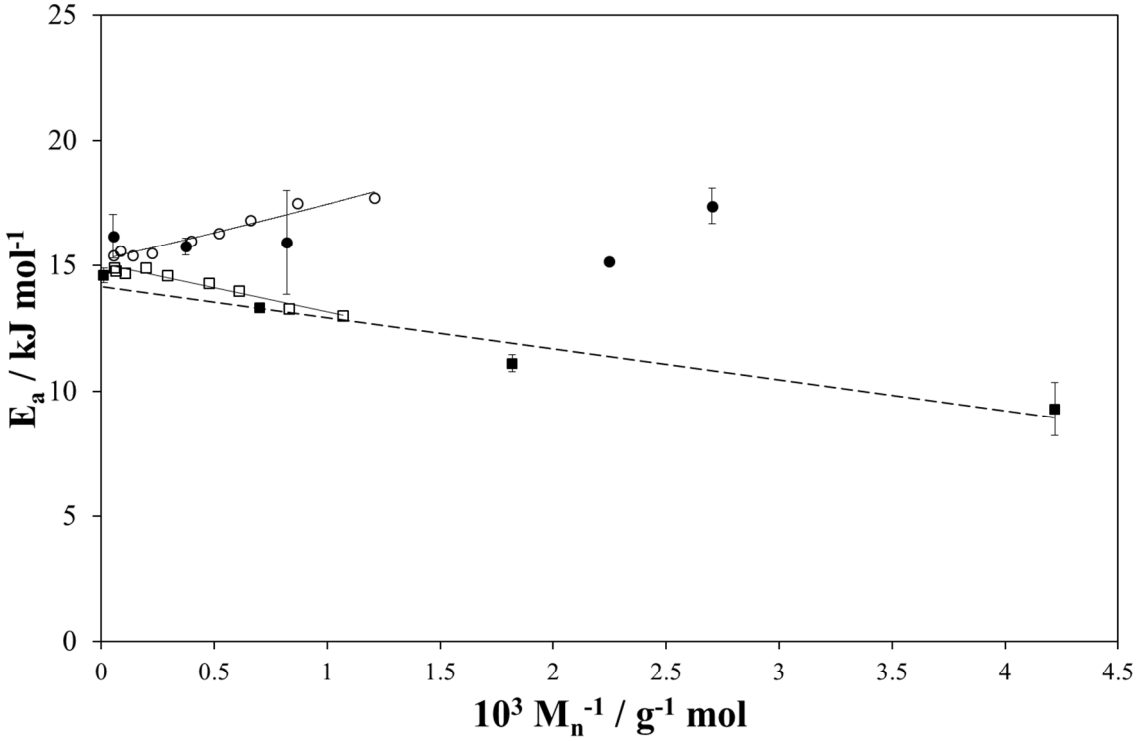

Figure 16 – Molar mass dependence of the activation energy for segmental motion as determined from data in Figure 15 using equation (26): linear PDMS (solid squares) and cyclic PDMS (solid circles). Experimental data are compared with activation energies of linear (open squares) and cyclic (open circles) PDMS from the rheological measurements reported in reference 10. Lines are guides to the eye.

Conclusion

A detailed investigation of local dynamics of linear and cyclic PDMS as a function of molar mass has been presented. QENS experiments in the time scale from 2 to 200 ps and at Q = 0.3 to 1.8 Å^{-1} were complemented by theoretical calculations carried out (a) within the framework of a freely-jointed (FJ) chain model devoid of any local correlation among the rotational states and

equivalent to a fully flexible bead-and-spring chain, and (b) for a realistic PDMS chain within the Rotational Isomerical State approach considering the monomeric -Si(CH_3)$_2$-O- as the repeat unit.

At low temperature, the experimental results show that the rotational motion of the methyl groups provides the main contribution to the quasielastic broadening. The $S(Q,\omega)$ data of cyclic PDMS can be represented by the same model used for linear chains[55, 56]. Our findings show that the methyl group rotation is described by the same parameters reported for a linear PDMS sample with M_w = 91700 g mol^{-1}, irrespective of molar mass and topology.

To extract information on segmental motion, a series of QENS measurements were carried out at temperatures above T_m i.e. in the melt state. Using the same procedure established for high molecular weight PDMS, we used a model function that explicitly accounts for contributions from methyl group rotation and segmental motion[55, 56]. For the segmental relaxation, measurements carried out at a constant distance from T_g show that the stretching exponent slightly decreases from $\beta \sim 0.6$ at low molar mass to values approaching 0.56 for linear chains. No clear evidence for differences between β values of linear and cyclic chains was found, within experimental error. We note that β values higher than 0.5 are predicted by theory and attributed to chain stiffness effects that increase with decreasing chain length.

Several features predicted by theory are also reproduced by the experimental data. Specifically, relaxation times of both linear and cyclic PDMS at temperatures equally distant from their T_gs increase with increasing molecular weight. Perhaps more importantly, rings display higher relaxation times for the segmental motion, i.e. relax at a slower rate, compared to linear chains of the same molar mass. This is true even when differences among glass transition temperatures are accounted for. Theoretical calculations support the idea that the topological constraint imposed by the ring closure slows down the local dynamics compared to a linear chain. For very large molar masses, this constraint becomes negligible and so the same τ_{eff} is achieved for both topologies. Interestingly, it is suggested by our calculations that, due to its conformational rigidity, PDMS undergoes an additional constraint which further increases τ_{eff} thus producing a shallow maximum for N ≈ 50 (Figure 4(*b*)).

Evidence for a broad maximum in τ_{eff} is also observed in the experimental QENS data (Figures 12 and 13).

Furthermore, the activation energy of cyclic PDMS is higher than that of linear chains, values being in reasonable agreement with viscosity measurements[10-12]. The pronounced molecular weight dependence of E_a for linear PDMS is primarily linked to the presence of mobile chain ends.

Our experiments and calculations based on siloxanes show changes with topology that are not only in agreement with previous QENS data[54] but also mimic the trend identified by both bulk viscosity measurements[10-12] as well as self-diffusion and spin-spin relaxation measurements[15] according to which rings have slower dynamics (higher viscosities or smaller diffusion coefficients) compared to linear chains at low molar mass but show opposite behaviour in the high molar mass range, above the entanglement molecular weight, M_e. Similar observations have been made by Ozisik *et al.*[75] and Hur *et al.*[25, 26] in their computer simulations of cyclic and linear polyethylenes. We note that experimental studies of ring dynamics have often been carried out on high molar mass samples, above M_e[38, 52, 76] and therefore the results are not comparable to our experimental data. However, for poly(oxyetheylene)s, Nam *et al.*[51] measured self-diffusion, NMR spin-spin relaxation and zero shear rate viscosities of monodisperse, of low molecular weight cyclic (400 to 1500 g mol^{-1}) and linear samples, reporting slower dynamics for rings.

As discussed in previous sections the faster motion of linear chains cannot be simply attributed to chain end effects; dynamic differences are still evident even after scaling at constant segmental mobility. Other effects such as frustration of segmental rotational diffusion in small rings and the configurational entropy of rings, which is generally much smaller than that of the linear chains[58], also need to be considered. As noted earlier, the observed slowing down of the segmental relaxation is attributed to the topological constraint imposed by the ring-closure which in turn slows down the intramolecular conformational rearrangements.

ACKNOWLEDGMENT.

We thank the ISIS (Rutherford Appleton Laboratory, UK) for beam time and Prof. P. Griffiths for kindly giving us some of the cyclic samples. We wish to acknowledge the important work

carried out over many years by the late Dr. J. A. Semlyen on cyclic polymers. Without his contribution, and that of his co-workers, this work would have not been possible.

References

1. Kricheldorf, H. R. *Journal of Polymer Science Part a-Polymer Chemistry* **2010,** 48, (2), 251-284.
2. Ungar, G.; Zeng, K. B. *Chem. Rev.* **2001,** 101, (12), 4157-4188.
3. Su, H.-H.; Chen, H.-L.; Diaz, A.; Teresa Casas, M.; Puiggali, J.; Hoskins, J. N.; Grayson, S. M.; Perez, R. A.; Mueller, A. J. *Polymer* **2013,** 54, (2), 846-859.
4. Clarson, S. J.; Dodgson, K.; Semlyen, J. A. *Polymer* **1985,** 26, (6), 930-934.
5. Huang, D. H.; Simon, S. L.; McKenna, G. B. *J Chem Phys* **2005,** 122, (8).
6. Dimarzio, E. A.; Guttman, C. M. *Macromolecules* **1987,** 20, (6), 1403-1407.
7. Liu, X. J.; Chen, D. L.; He, Z. D.; Zhang, H.; Hu, H. Z. *Polymer Communications* **1991,** 32, (4), 123-125.
8. Gan, Y. D.; Dong, D. H.; Hogenesch, T. E. *Macromolecules* **1995,** 28, (1), 383-385.
9. Santangelo, P. G.; Roland, C. M.; Chang, T.; Cho, D.; Roovers, J. *Macromolecules* **2001,** 34, (26), 9002-9005.
10. Dodgson, K.; Bannister, D. J.; Semlyen, J. A. *Polymer* **1980,** 21, (6), 663-667.
11. Orrah, D. J.; Semlyen, J. A.; Rossmurphy, S. B. *Polymer* **1988,** 29, (8), 1452-1454.
12. Orrah, D. J.; Semlyen, J. A.; Rossmurphy, S. B. *Polymer* **1988,** 29, (8), 1455-1458.
13. Mills, P. J.; Mayer, J. W.; Kramer, E. J.; Hadziioannou, G.; Lutz, P.; Strazielle, C.; Rempp, P.; Kovacs, A. J. *Macromolecules* **1987,** 20, (3), 513-518.
14. Tead, S. F.; Kramer, E. J.; Hadziioannou, G.; Antonietti, M.; Sillescu, H.; Lutz, P.; Strazielle, C. *Macromolecules* **1992,** 25, (15), 3942-3947.
15. Cosgrove, T.; Griffiths, P. C.; Hollingshurst, J.; Richards, R. D. C.; Semlyen, J. A. *Macromolecules* **1992,** 25, (25), 6761-6764.
16. Cosgrove, T.; Turner, M. J.; Griffiths, P. C.; Hollingshurst, J.; Shenton, M. J.; Semlyen, J. A. *Polymer* **1996,** 37, (9), 1535-1540.
17. Zimm, B. H.; Stockmayer, W. H. *The journal of chemical physics* **1949,** 17, 1301.
18. Casassa, E. F. *Journal of Polymer Science, Part A* **1965,** 3, 605.
19. Burchard, W.; Schmidt, M. *Polymer* **1980,** 21, (7), 745-749.
20. Cates, M. E.; Deutsch, J. M. *Journal De Physique* **1986,** 47, (12), 2121-2128.
21. Klein, J. *Macromolecules* **1986,** 19, (1), 105-118.
22. Brown, S.; Szamel, G. *J Chem Phys* **1998,** 109, (14), 6184-6192.
23. Brown, S.; Szamel, G. *J Chem Phys* **1998,** 108, (12), 4705-4708.
24. Deutsch, J. M. *Phys Rev E* **1999,** 59, (3), R2539-R2541.
25. Hur, K.; Jeong, C.; Winkler, R. G.; Lacevic, N.; Gee, R. H.; Yoon, D. Y. *Macromolecules* **2011,** 44, (7), 2311-2315.
26. Hur, K.; Winkler, R. G.; Yoon, D. Y. *Macromolecules* **2006,** 39, (12), 3975-3977.
27. Suzuki, J.; Takano, A.; Matsushita, Y. *J Chem Phys* **2008,** 129, (3).
28. Suzuki, J.; Takano, A.; Deguchi, T.; Matsushita, Y. *J Chem Phys* **2009,** 131, (14).
29. Muller, M.; Wittmer, J. P.; Cates, M. E. *Phys Rev E* **1996,** 53, (5), 5063-5074.
30. Higgins, J. S.; Dodgson, K.; Semlyen, J. A. *Polymer* **1979,** 20, (5), 553-558.

31. Edwards, C. J. C.; Richards, R. W.; Stepto, R. F. T.; Dodgson, K.; Higgins, J. S.; Semlyen, J. A. *Polymer* **1984,** 25, (3), 365-368.
32. Roovers, J.; Toporowski, P. M. *Macromolecules* **1983,** 16, (6), 843-849.
33. Roovers, J. *Macromolecules* **1985,** 18, (6), 1359-1361.
34. Takano, A.; Ohta, Y.; Masuoka, K.; Matsubara, K.; Nakano, T.; Hieno, A.; Itakura, M.; Takahashi, K.; Kinugasa, S.; Kawaguchi, D.; Takahashi, Y.; Matsushita, Y. *Macromolecules* **2012,** 45, (1), 369-373.
35. Takano, A.; Kushida, Y.; Ohta, Y.; Masuoka, K.; Matsushita, Y. *Polymer* **2009,** 50, (5), 1300-1303.
36. Arrighi, V.; Gagliardi, S.; Dagger, A. C.; Semlyen, J. A.; Higgins, J. S.; Shenton, M. J. *Macromolecules* **2004,** 37, (21), 8057-8065.
37. Gagliardi, S.; Arrighi, V.; Ferguson, R.; Dagger, A. C.; Semlyen, J. A.; Higgins, J. S. *J Chem Phys* **2005,** 122, (6).
38. Bras, A. R.; Pasquino, R.; Koukoulas, T.; Tsolou, G.; Holderer, O.; Radulescu, A.; Allgaier, J.; Mavrantzas, V. G.; Pyckhout-Hintzen, W.; Wischnewski, A.; Vlassopoulos, D.; Richter, D. *Soft Matter* **2011,** 7, (23), 11169-11176.
39. Beaucage, G.; Kulkarni, A. S. *Macromolecules* **2010,** 43, (1), 532-537.
40. de Gennes, P.-G. *The journal of chemical physics* **1971,** 55, 572.
41. Doi, M.; Edwards, S. *J. Chem. Soc., Faraday Trans. 2* **1978,** 74, 1789-1801.
42. Doi, M.; Edwards, S. *Journal of the Chemical Society, Faraday Transactions 2: Molecular and Chemical Physics* **1978,** 74, 1802-1817.
43. Doi, M.; Edwards, S. *J. Chem. Soc., Faraday Trans. 2* **1979,** 75, 38-54.
44. Klein, J.; Fletcher, D.; Fetters, L. J. *Nature* **1983,** 304, (5926), 526-527.
45. Hild, G.; Strazielle, C.; Rempp, P. *Eur Polym J* **1983,** 19, (8), 721-727.
46. Mckenna, G. B.; Plazek, D. J. *Abstr Pap Am Chem S* **1987,** 193, 161-POLY.
47. Kapnistos, M.; Lang, M.; Vlassopoulos, D.; Pyckhout-Hintzen, W.; Richter, D.; Cho, D.; Chang, T.; Rubinstein, M. *Nature Materials* **2008,** 7, (12), 997-1002.
48. McKenna, G. B.; Hostetter, B. J.; Hadjichristidis, N.; Fetters, L. J.; Plazek, D. J. *Macromolecules* **1989,** 22, (4), 1834-1852.
49. Kawaguchi, D.; Masuoka, K.; Takano, A.; Tanaka, K.; Nagamura, T.; Torikai, N.; Dalgliesh, R. M.; Langridge, S.; Matsushita, Y. *Macromolecules* **2006,** 39, (16), 5180-5182.
50. Roovers, J. *Macromolecules* **1988,** 21, (5), 1517-1521.
51. Nam, S.; Leisen, J.; Breedveld, V.; Beckham, H. W. *Polymer* **2008,** 49, (25), 5467-5473.
52. Richter, D.; Goossen, S.; Wischnewski, A. *Soft Matter* **2015,** 11, (44), 8535-8549.
53. Ganazzoli, F.; Raffaini, G.; Arrighi, V. *Phys Chem Chem Phys* **2002,** 4, (15), 3734-3742.
54. Allen, G.; Brier, P. N.; Goodyear, G.; Higgins, J. S. *Faraday Symp Chem S* **1972,** 6, (0), 169-175.
55. Arrighi, V.; Gagliardi, S.; Zhang, C. H.; Ganazzoli, F.; Higgins, J. S.; Ocone, R.; Telling, M. T. F. *Macromolecules* **2003,** 36, (23), 8738-8748.
56. Arrighi, V.; Ganazzoli, F.; Zhang, C. H.; Gagliardi, S. *Phys Rev Lett* **2003,** 90, (5).
57. Grapengeter, H. H.; Alefeld, B.; Kosfeld, R. *Colloid Polym Sci* **1987,** 265, (3), 226-233.
58. Kirst, K. U.; Kremer, F.; Pakula, T.; Hollingshurst, J. *Colloid Polym Sci* **1994,** 272, (11), 1420-1429.
59. Roland, C. M.; Nagi, K. L. *Macromolecules* **1996,** 29, (17), 5747-5750.

60. Goodwin, A. A.; Beevers, M. S.; Clarson, S. J.; Semlyen, J. A. *Polymer* **1996,** 37, (13), 2597-2602.
61. Goodwin, A. A.; Beevers, M. S.; Clarson, S. J.; Semlyen, J. A. *Polymer* **1996,** 37, (13), 2603-2607.
62. Smith, J. S.; Borodin, O.; Smith, G. D. *J Phys Chem B* **2004,** 108, (52), 20340-20350.
63. Allen, G.; Higgins, J. S.; Wright, C. J. *J Chem Soc Farad T 2* **1974,** 2, (70), 348-355.
64. Cowie, J.; McEwen, I. *Polymer* **1973,** 14, (9), 423-426.
65. Allegra, G.; Ganazzoli, F. *J Chem Phys* **1981,** 74, (2), 1310-1320.
66. Perico, A.; Ganazzoli, F.; Allegra, G. *J Chem Phys* **1987,** 87, (6), 3677-3686.
67. Akcasu, A. Z.; Benmouna, M.; Han, C. C. *Polymer* **1980,** 21, (8), 866-890.
68. Bée, M., *Quasielastic neutron scattering : principles and applications in solid state chemistry, biology and materials science*. A. Hilger: Bristol; Philadelphia, 1988.
69. Chahid, A.; Alegria, A.; Colmenero, J. *Macromolecules* **1994,** 27, (12), 3282-3288.
70. Frick, B.; Fetters, L. J. *Macromolecules* **1994,** 27, (4), 974-980.
71. Ngai, K. L.; Colmenero, J.; Alegria, A.; Arbe, A. *Macromolecules* **1992,** 25, (24), 6727-6729.
72. Colmenero, J.; Alegria, A.; Alberdi, J. M.; Alvarez, F.; Frick, B. *Phys Rev B* **1991,** 44, (14), 7321-7329.
73. Alvarez, F.; Arbe, A.; Colmenero, J. *Chem Phys* **2000,** 261, (1-2), 47-59.
74. Frick, B.; Dosseh, G.; Cailliaux, A.; Alba-Simionesco, C. *Chem Phys* **2003,** 292, (2-3), 311-323.
75. Ozisik, R.; von Meerwall, E. D.; Mattice, W. L. *Polymer* **2002,** 43, (2), 629-635.
76. Bras, A. R.; Goossen, S.; Krutyeva, M.; Radulescu, A.; Farago, B.; Allgaier, J.; Pyckhout-Hintzen, W.; Wischnewski, A.; Richter, D. *Soft Matter* **2014,** 10, (20), 3649-3655.

Graphical Abstract